Supporting Information for

In situ generation of cellulose nanocrystals in polycaprolactone nanofibers: Effects on crystallinity, mechanical strength, biocompatibility, and biomimetic mineralization

Mahesh Kumar Joshi[1, 2], Arjun Prasad Tiwari[1], Hem Raj Pant[3], Bishnu Kumar Shrestha[1], Han Joo Kim[1,4], Chan Hee Park[1*], Cheol Sang Kim[1, 5, 6*]

[1]Department of Bionanosystem Engineering, Graduate School, Chonbuk National University, Jeonju 561-756, Republic of Korea

[2]Department of Chemistry, Tri-Chandra Multiple Campus, Tribhuvan University, Kathmandu, Nepal

[3]Department of Engineering Science and Humanities, Institute of Engineering, Pulchowk Campus, Tribhuvan University, Kathmandu, Nepal

[4]Department of Convergence Technology Engineering, College of engineering, Chonbuk National University, Jeonju 561-756, Republic of Korea

[5]Division of Mechanical Design Engineering, Chonbuk National University, Jeonju 561-756, Republic of Korea

[6]Eco-friendly machine parts design research center, Chonbuk National University, Jeonju 561-756, Republic of Korea

*Corresponding authors: Tel.: +82-63-270-4284; fax: +82-63-270-2460.

E-mail: chskim@jbnu.ac.kr (C. S. Kim), biochan@jbnu.ac.kr (C.H Park)

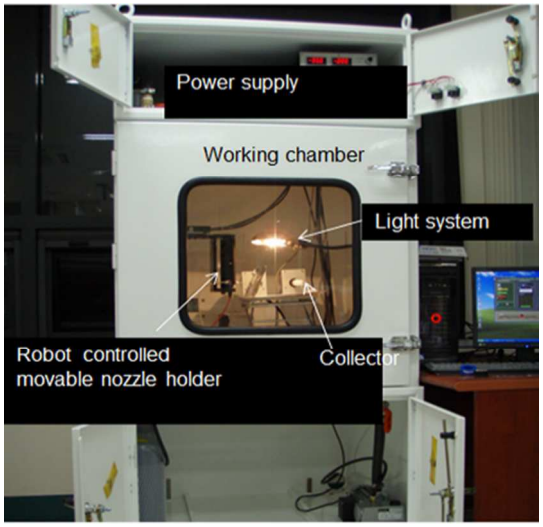

Figure. S1. Digital image of electrospinning setup used in this study

Fiber diameter distribution.

Figure S2 shows the bar diagram for fiber diameter distribution in different mats. However, there was no significant difference in fiber diameter of different mats, the average fiber diameter and the standard deviation were slightly decreased from MR1 to MR4. This result shows that that the more uniform fibers were obtained at higher composition of PCL in nanofibers

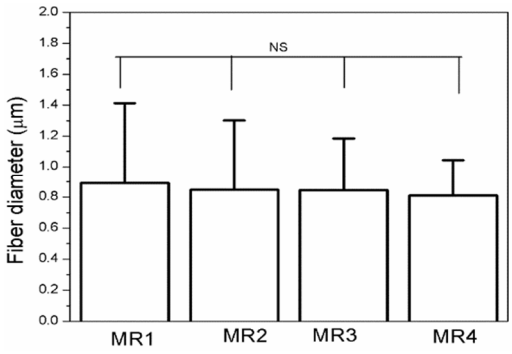

Figure S2. Bar diagram showing the fiber diameter distributions in different mats. No significance difference was observed (one-way ANOVA, $p<0.05$)

Evaluation of FT-IR spectra of different scaffolds

Figure S3 shows the FT-IR spectra of different scaffolds types. The absorption bands corresponding to C–O–C stretching of cellulose acetate at 1037 and 1229 cm^{-1} were steadily narrowed from M1 to M4 mat (Fig. S3A). Additionally, the peak at 1741 cm^{-1} was shifted to 1755 cm^{-1} with increasing PCL composition in the fibrous matrix. When the mats were treated with NaOH solution, the acetyl group was completely removed as indicated by the FT-IR spectra of treated mat (Fig. S3B). The PCL content in the composite fiber was not affected by the alkaline saponification (since absorption bands related to PCL remained unchanged). The absorption bands at 1229 cm^{-1} and 1755 cm^{-1} related to the acetyl group and carbonyl group of cellulose acetate, respectively, were disappeared in the spectrum of the treated mats (Fig. S3B). These results indicated the complete hydrolysis of cellulose acetate into cellulose.

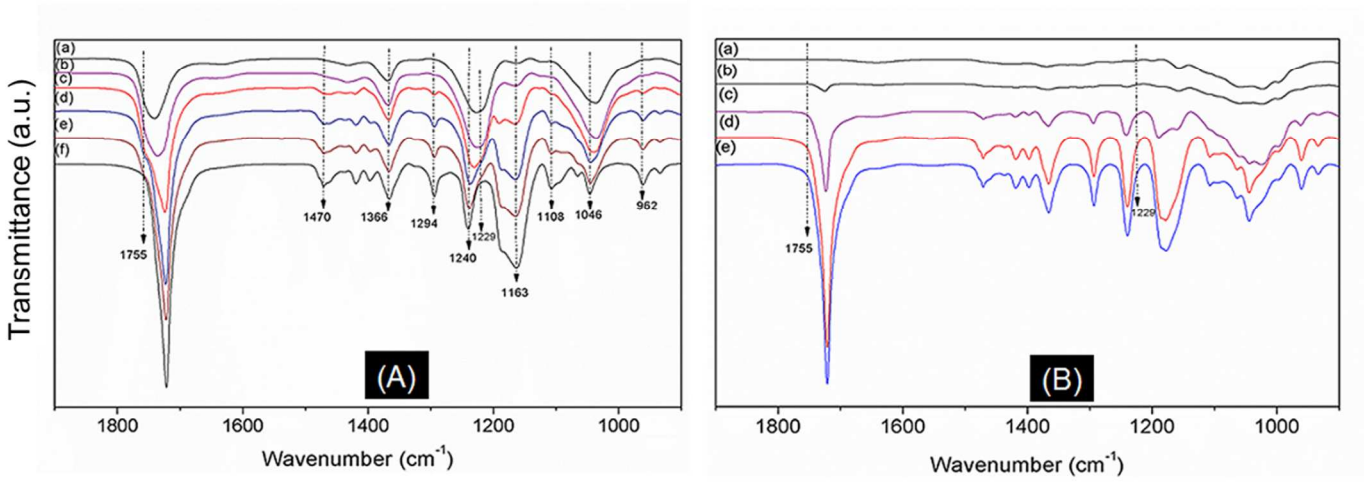

Figure S3. (A) FTIR spectra of (a) pristine CA mat, (b) M1, (c) M2, (d) M3, (e) M4, (f) pristine PCL mat. (B) FTIR spectra after saponification (a) regenerated cellulose, (b) MR1, (c) MR2, (d) MR3, and (e) MR4.

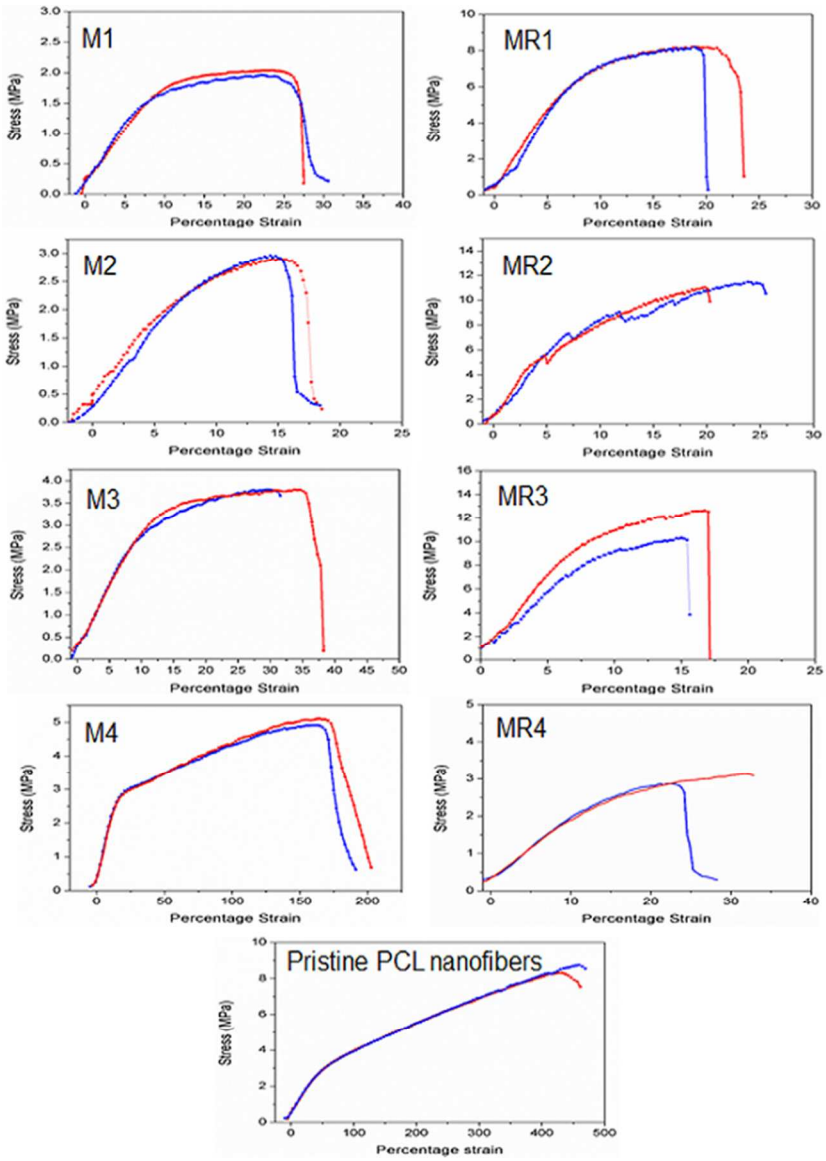

Figure S4. Tensile stress-strain curves for different mats.

TEM Images

Electrospun nanofibers, PCL/CA (M3), were directly collected in a TEM grid and TEM image was taken. In case of PCL/CL nanofiber, firstly, nanofibers were collected in TEM grid and then treated with 0.05M NaOH (prepared in 4:1 ethanol/water mixed solvent system) for 24 h and carefully rinsed with distilled water, dried and TEM image was taken.

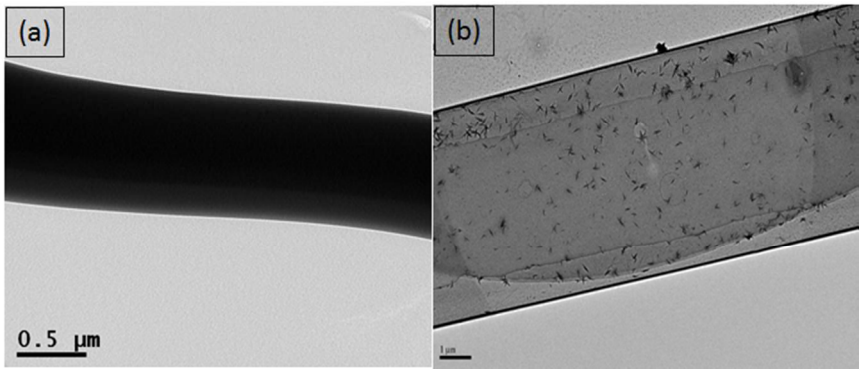

Figure S5. TEM images of (a) PCL/CA (M3) nanofiber and (b) corresponding PCL/CL (MR3) nanofiber

Wettability of composite mats

Along with the water contact angle, wettability was also evaluated non-polar liquid diiodomethane and polar liquid glycerol. All PCL/CA mats (M1 to M4) showed zero degree contact angle for diiodomethane and nearly about 136 degree for glycerol indicating the hydrophobic surface, similar to the water contact angle. After saponification, the contact angle for diiodomethane was gradually decreased while that for glycerol was increased, similar to the water contact angle. The increase in contact angle for glycerol and water is attributed to the gradual increase in composition of PCL and decrease in composition of CL from MR1 to MR4. Decrease in CL composition means decrease in the numbers of polar OH groups in the nanofiber. Consequently, the wettability for polar liquids glycerol decreased and contact angle increased.

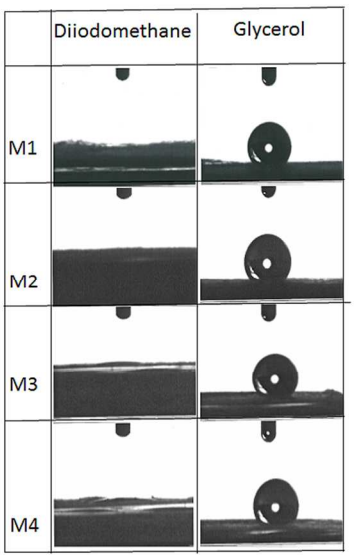

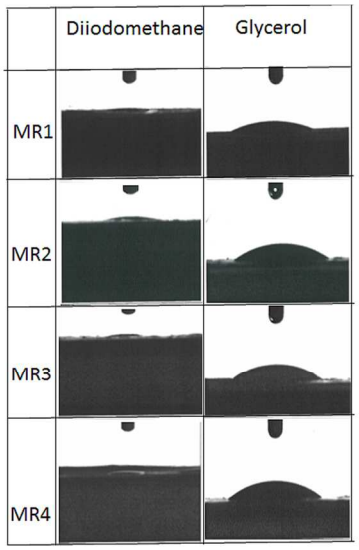

Sample	Contact angle for Diiodomethane (Degree)	Contact angle for Glycerol (Degree)
M1	0	135.5
M2	0	136.5
M3	0	135.5
M4	0	137
MR1	18.8	24.7
MR2	15.5	28.2
MR3	10.2	32.2
MR4	8.5	34.4

Figure S6. Contact angle for different mats using diiodomethane and glycerol.

Wettability of electrospun PCL mat

The biomimetic mineralization of the electrospun nanofibrous mat was effected by the wettability or solution absorption properties of the polymer. Contact angle measurement is the suitable technique to measure the wettability of the electrospun mat. The PCL nanofibrous mat showed the surface deposition of calcium phosphate compound. The water contact angle measurement for PCL mat was found to be 125.8^{o} (Fig. S7) indicating its hydrophobic nature. When the mat was incubated in SBF solution, the inner fibers did not showed the biomimetic mineralization which is attributed to its hydrophobic nature that inactivate the capillaries as a result solution con not reach up to the inner fibers.

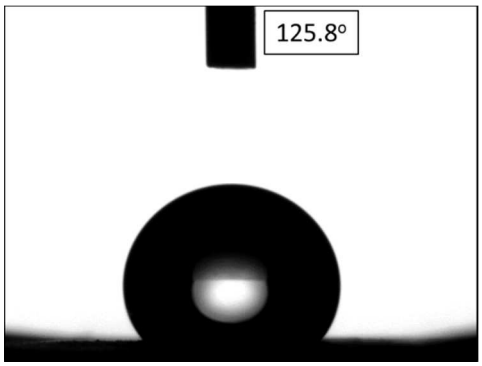

Figure. S7. Water contact angle images of PCL mats.

Fabrication and biomimetic mineralization of regenerated cellulose mat

Cellulose acetate (CA) solution (17 Wt %) was prepared by dissolving in a solvent system of acetone and N-dimethylacetamide (2:1wt %) under magnetic stirring for 12 h at room temperature according to previous report [1]. The solution (about 8 mL) was drawn into 12 mL plastic syringe connected with metal capillary through a plastic tube. The syringe was fixed onto a syringe pump where the flow rate was maintained at 1 mL/h. Electrospinning was carried out at room condition (temperature = 18 °C, and humidity = 30 %), 17 kV applied voltage and 15 cm tip-to-collector distance. The fibers were collected aluminum sheet attached to the rotating iron drum. The electrospun mat was carefully removed from the aluminum sheet and immersed into 0.05 M NaOH in H_2O/ethanol (1:4 v/v) solution for 24 h at room temperature in order to remove acetyl group via alkali catalyzed saponification [2]. Resulting cellulose mat was thoroughly rinsed with distilled water until the wash solution becomes neutral.

To compare the biomimetic mineralization ability of cellulose acetate and regenerated cellulose mat, both mats were incubated in SBF solution. SBF solution was prepared according to our previous report [3]. Briefly, commercially available

Hank's balance salt (Aldrich, H2387-1) was dissolved in 1L aqueous solution along with, 0.097g of $MgSO_4$, 0.350g of $NaHCO_3$, and 0.185g of $CaCl_2$.

Cellulose acetate and regenerated cellulose mat were cultured in the SBF solution for different time intervals. Figure. S8 shows the surface morphology of the five days mineralized scaffolds. In case of cellulose acetate (Fig. S8a), small particles were deposited the random area along the fiber surface while kalopanax bark like HAp particles were deposited throughout the fiber surface, suggesting that the cellulose mat can induce crystal formation under SBF treatment which might be from the carboxylate groups formed during the slight oxidative degradation during alkaline saponification or it might be from active hydroxyl groups on the cellulose nanofibers [1]. An energy dispersive X-ray spectroscopy connected to FE-SEM demonstrated that the mole ratio of Ca/P is 1.58 (Fig. S9), which is less than 1.67 of natural bone [4]. This result suggests that the HAp on cellulose nanofiber is calcium deficient and effective for bone regeneration applications. It is believed that the hydroxyl functionality on the cellulose mat may firstly bind the calcium ions through ionic dipolar interaction and then hydroxyapatite grow around these trapped ions [5].

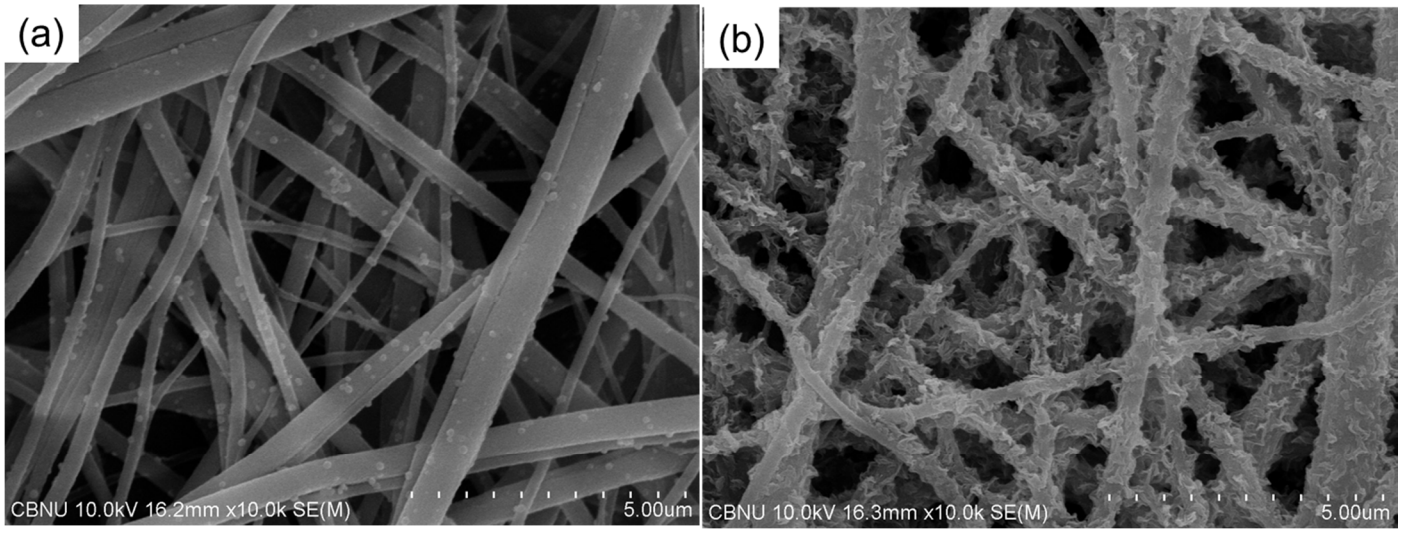

Figure. S8. FE-SEM images of five days mineralized cellulose acetate mat (a) and regenerated cellulose mat (b).

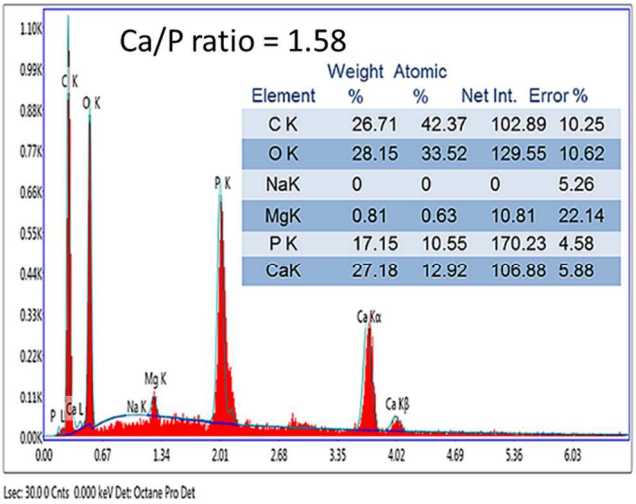

Figure. S9. EDX spectra of ten days mineralized regenerated cellulose mat.

References

1. Rodríguez, K.; Renneckar, S.; Gatenholm, P. Biomimetic Calcium Phosphate Crystal Mineralization on Electrospun Cellulose-Based Scaffolds. *ACS Appl. Mater. Interfaces* **2011,** *3*, 681-689.
2. Ma, Z.; Kotaki, M.; Ramakrishna, S. Electrospun cellulose nanofiber as affinity membrane. *J. Membr. Sci.* **2005,** *265*, 115-123.
3. Joshi, M. K.; Pant, H. R.; Tiwari, A. P.; kim, H. J.; Park, C. H.; Kim, C. S. Multi-layered macroporous three-dimensional nanofibrous scaffold via a novel gas foaming technique. *Chem. Eng. J. (Amsterdam, Neth.)* **2015,** *275*, 79-88.
4. Hutchens, S. A.; Benson, R. S.; Evans, B. R.; O'Neill, H. M.; Rawn, C. J. Biomimetic synthesis of calcium-deficient hydroxyapatite in a natural hydrogel. *Biomaterials* **2006,** *27*, 4661-4670.
5. Wan, Y. Z.; Huang, Y.; Yuan, C. D.; Raman, S.; Zhu, Y.; Jiang, H. J.; He, F.; Gao, C. Biomimetic synthesis of hydroxyapatite/bacterial cellulose nanocomposites for biomedical applications. *Mater. Sci. Eng., C* **2007,** *27*, 855-864.